# Viewpoint-Invariant Representation of Generalized Cylinders Using the Symmetry Set

Nic Pillow, Sven Utcke and Andrew Zisserman
Robotics Research Group, Department of Engineering Science
Oxford University, OX1 3PJ.

**Abstract**

We demonstrate that viewpoint-invariant representations can be obtained from images for a useful class of 3D smooth object. The representations are stable over viewpoint, and also discriminate between different objects in the same class. They are computed using only image information, from the symmetry set of the object's outline.

Examples are given of the representations obtained from real perspective images, and their use in a model-based recognition system for canal surfaces.

## 1 Introduction

The aim of this work is to extract viewpoint-invariant descriptions of 3D smooth objects from single images. These descriptions are used as shape descriptors in a model-based recognition system. For a completely general object, and with no other information, it is not possible to recover shape or invariant descriptions from a single image (see for example [6, 8, 15] for 3D point sets). However, if the 3D structure is *constrained*, then invariant descriptions can be obtained. Here we consider surfaces belonging to a particular class of generalized cylinder (GC) [1]. The class consists of surfaces generated as the envelope of a *sphere* of varying radius swept along the cylinder axis (which need not be straight). Examples include pipes or tubes ('canal surfaces') where the sphere radius is constant, and surfaces of revolution, where the axis is a line. This class generates a large number of commonly occurring manufactured objects.

The key idea here is that since the 'envelope of the profile[1] is the profile of the envelope' the image projection is an envelope of circles. By inverting this process—recovering circles from the profile—the projection of the axis and the scaling function can be extracted from the image.

Previous work on extracting this class of GC from images has had different or more limited goals: first, rather than perspective, the weak perspective imaging approximation is generally used (see [19, 27], where earlier

[1]The image outline of the surface.

BMVC 1994 doi:10.5244/C.8.53

references are given); second, the goal has been reconstruction rather than representation, and this requires a reference cross-section to be visible in the image [25]; third, those methods that do produce invariants under perspective [10] only utilize a number of points on the image outline—not the entire curve. In this paper, in common with the above, only the profile is used; no use is made of surface markings or texture.

The tool employed here is the *symmetry set*, studied by Giblin & Brassett [11], which is the locus of centres of circles bitangent to a plane curve. Previous symmetry analysis has largely concentrated on extracting bilateral (reflection) or rotational symmetries from images of planar objects, or from a single silhouette of 3D objects, viewed in a fronto-parallel plane [3, 4, 23]. The methods developed for those cases can not be applied if the viewpoint is not fronto-parallel since, for a planar object, reflectional symmetries are then *skewed* by imaging [12, 17, 26]. For a 3D smooth object additional distortions occur—the contour generator[2] moves on the surface as viewing position changes. In this case it is not a fixed space curve which is projected, and the image profile can change radically with viewpoint, defeating any simple application of skewed symmetry.

# 2 Theory

In the following we consider two types of image projection: perspective and weak perspective. In both cases the camera aspect ratio must be known, though no other intrinsic parameters are required. However, much of the construction uses only affine or projective properties; this is made explicit.

## 2.1 Weak perspective

Consider sweeping a sphere of varying radius along the axis curve; the resulting surface is the envelope of the swept sphere. At each point the profile of the sphere is a circle, and the profile of the surface is the envelope of the circles. Under affine projection the centre of the sphere projects to the centre of the circle. Consequently, the circle's centre sweeps out the projection of the axis. Now consider two such circles: as the scaling arising from weak perspective is the same in both cases, the ratio of circle radii equals the ratio of radii of the generating spheres. The usefulness of these results is that the circle can be recovered from the profile by constructing the symmetry set, the locus of centres of circles bitangent to the profile. To summarize:

[2] The curve on the surface which projects to the image profile.

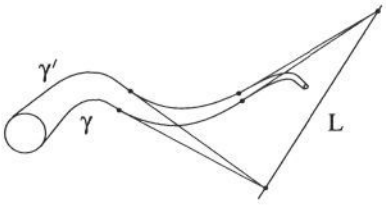


Figure 1: *For a canal surface with a planar axis, inflections in the profile occur in pairs for each inflection of the axis. The intersection of a pair of inflection tangents determines the vanishing point of the tangent line at the axis inflection. Two such vanishing points determine the vanishing line, L, of the plane of the axis.*

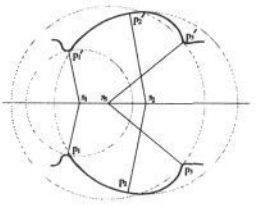

Figure 2: *Three fitted circles for a surface of revolution. Note that the centre's position on the axis of symmetry, s, is not a monotonic function of distance along the profile, p. This problem does not occur for canal surfaces.*

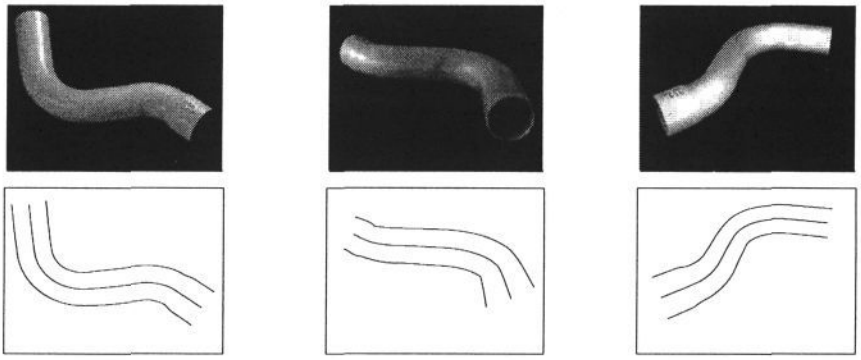

Figure 3: *Upper: images from substantially different viewpoints of the same generalized cylinder (pipe 1). Lower: the profiles and extracted symmetry sets. Note the radically different shapes of the profiles and symmetry sets. However, in a canonical frame the three symmetry sets are virtually identical—see figure 4c.*

*Given a weak perspective image of a surface generated as the envelope of a sphere of varying radius $R(S)$, with centres on a plane curve $\alpha(S)$ (the axis); the symmetry set, computed from the image profile, has the following properties: (1) the contact of image circles with the profile identifies corresponding points on the surface, i.e. points which lie on the same circular cross-section; (2) the curve covered by circle centres, $\sigma(s)$, is within a plane affine transformation of the curve $\alpha(S)$; (3) the scaling function for radii of image circles, $r(s)$, equals the scaling function for radii of the generating spheres $R(S)$ for corresponding points, $\alpha(S)$ and $\sigma(s)$, up to an overall scale ambiguity.*

The curves $\{\sigma(s), r(s)\}$ are a viewpoint-invariant representation. $\alpha(S)$ is determined up to an affine ambiguity, and consequently affine invariants of $\alpha(S)$ are equal to affine invariants of $\sigma(s)$, and these are viewpoint-invariant. $R(S)$ is determined up to scale.

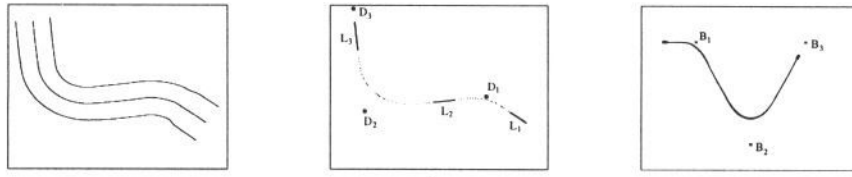


Figure 4: *The transformation of a symmetry set into an affine canonical frame. (a) Profile curves and symmetry set obtained from a weak perspective image. (b) Distinguished lines and their intersections, the three distinguished points. The transformation is found which maps the distinguished points,* $\{\mathbf{D}_1, \mathbf{D}_2, \mathbf{D}_3\}$*, onto the basis points,* $\{\mathbf{B}_1, \mathbf{B}_2, \mathbf{B}_3\}$ *(the vertices of an isosceles triangle). (c) The result of applying this transformation to the whole symmetry set. The basis points are shown as crosses. There are six symmetry sets superimposed here. These are extracted from weak perspective images with varying viewpoint of pipe 1 (three from figure 3 and three similar). They are virtually identical, demonstrating the stability of the affine frame.*

## 2.2 Perspective

Under perspective projection the profile of a sphere is an ellipse, and the centre of the sphere does not project to the ellipse centre. However, in practice, for finite image planes this effect is extremely small: the aspect ratio of a sphere's profile is at worst 0.94, and its centre is displaced at most by 1.2% of its diameter, even at the border of a wide-angle lens with $46^o$ field of view. This is an example of a *quasi-invariant* [2]. Thus, the symmetry set will still be an excellent approximation of the projected axis. However, the transformation between a planar axis curve and symmetry set curve will be projective, rather than affine. It is shown in section 4.2 that for canal surfaces with at least two inflections, $\alpha(S)$ is determined up to an affine ambiguity, even under perspective distortion.

## 2.3 Canal Surfaces

Here there is an additional constraint that the scaling function is a constant. A canal surface has a number of properties which do not hold for a general GC of this class: (1) Under weak perspective projection, the two sides of the profile are parallel curves of the symmetry set (the projection of the axis). This follows directly from the profile curves being the envelope of constant-radius circles swept along the symmetry set. (2) Inflections in the axis produce inflection pairs on the profile. Tangents at corresponding profile inflections (on each side of the profile) intersect on the vanishing line of the axis curve's plane. Two such intersections determine the vanishing line, and hence the extraction of affine curve measurements; see figure 1. This relationship is exact—it is not a quasi-invariant. Note: this constraint also

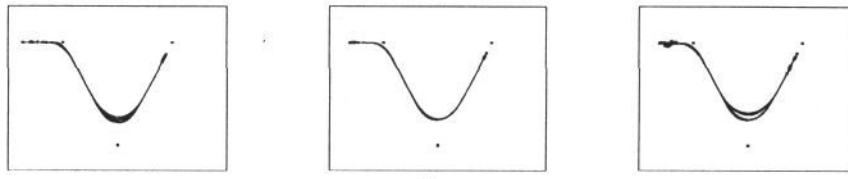

a b c

Figure 5: *(a) Affine canonical frame for symmetry sets from six weak perspective images (as in figure 4c) and seven images with significant perspective effects. Note the distortion for the latter curves. (b) Projective canonical frame for thirteen images of the same pipe used in (a). The curves are virtually identical, eliminating the perspective distortion shown in the affine frame. (c) Superimposed symmetry sets of pipes 1 and 4 (pipe 4 is shown in figure 6) in a projective canonical frame. In each case there are twelve curves. This demonstrates discrimination between objects from their canonical frame curves. The difference between the two curve sets is measured using a statistical classifier.*

applies to line segments on the profile (a line is a 'degenerate' inflection), so can be applied to a piecewise linear axis.

# 3 Extracting the Symmetry Set

Edges are extracted to sub-pixel accuracy using a local implementation of the Canny edge operator [7]. These are linked into edgel-chains by a sequential linker which extrapolates over small gaps. Accurate curve normals are computed at each point of the edgel-chain, by locally fitting a quadratic using least squares with central Gaussian weighting on a thirteen point neighbourhood. Bitangent circles are obtained by simultaneously moving along paired curves. Corresponding points are identified if their normal has an equal angle with the chord linking the points. Circles are fitted to the thirteen point profile neighbourhood of the corresponding points using Pratt's circle fitting algorithm [20]. Further details are given in [18]. Figure 2 illustrates the parametrization problem for the symmetry set of a surface of revolution. Examples of extracted symmetry sets for canal surfaces are shown in figure 3.

# 4 Viewpoint-Invariant Representation: The Canonical Frame Construction

A canonical frame is a method of affine [13] or projective [21] curve normalization. The normalization is achieved in two stages. First, a number of *distinguished points* (or lines) are selected on the curve. Distinguished points are ones which can be located before and after the transformation,

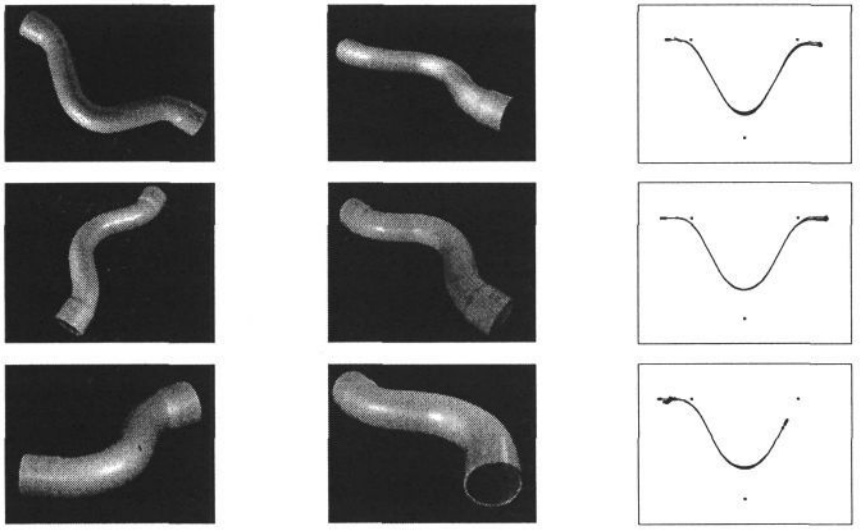

Figure 6: *Example images and projective canonical frames for three generalized cylinders, pipes 2, 3 and 4. Note the wide variation in viewing position. From top to bottom, the canonical frames contain symmetry sets generated from six, five and twelve images respectively. At least half of each set show significant perspective distortions—note the variation in pipe width in the middle column due to perspective. The end-diameter of pipe 2 is 15mm—the same diameter as pipe 1; pipes 3 and 4 both have an end-diameter of 22mm.*

such as corners (tangent discontinuities), inflections (zeros of curvature), and bitangent contact points. Second, the canonical frame is defined by selecting positions for a number of basis points or lines, for instance, the three vertices of an equilateral triangle in the affine case. The curve is then transformed such that the distinguished points map to the basis points. All curves which are equivalent up to an affine transformation map to the same curve. In the projective case, four points or lines are required.

## 4.1 Affine Frame

Figures 4a–c show the distinguished lines and points for the pipes, and the transformation to a canonical frame. For weak perspective images, stability over viewpoint is excellent; see figure 4c.

## 4.2 Projective Frame

In general, an axis curve can only be recovered up to a projective transformation from a perspective image. However, for canal surfaces, the vanishing line of the axis curve plane can be determined from profile inflection tangents by the construction of figure 1, and hence the projective ambiguity reduced to affine. The projective transformation to the canonical frame

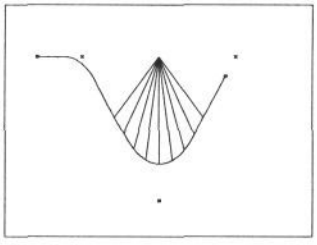

Figure 7: *The construction used to obtain the invariant line lengths* **L** *in the canonical frame. Nine rays are cast from a point mid-way between two of the distinguished points. The value recorded is the length of the ray. The rays have equal angular separation.*

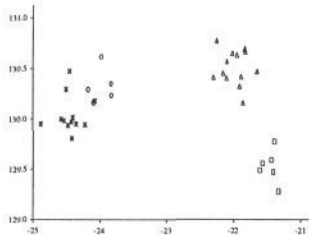


Figure 8: *Scatter plot of the first two invariants computed from the pipe images. Pipes 1–4 are represented by triangles, squares, circles and stars respectively. This demonstrates the sensitivity of the discriminant—the canonical frame curves for pipes 1 & 2 are almost identical.*

is computed from the following two requirements: first, the vanishing line maps to infinity; second, the three distinguished points are mapped to the affine canonical frame basis points.

Stability is poor if an affine frame (three symmetry set lines) is used for perspective images, see figure 5a. However, if a projective frame (three symmetry set lines and the vanishing line) is used, stability is excellent; see figure 5b. Examples of projective frames for other pipes and discrimination between them are given in figures 5c and 6.

# 5 Viewpoint-Invariant Measurements: Invariants

The previous section described the computation of viewpoint-invariant *curves*. Here, we compute *invariants* from the curves. An invariant is a number whose value is unaffected by viewpoint. Invariants are obtained from measurements on the canonical frame curve illustrated in figure 7. This construction [22] is similar to the *footprints* of Lamdan, *et al.* [13], although here lengths are measured rather than areas. The vector of invariant line lengths **L** is not used directly for discrimination. Instead, an *index vector* **M** is constructed from **L** using a statistical classifier (a Fisher linear discriminant [9]) over all extracted canonical frame curves.

Values of these invariants and their variances for the four pipes of figures 3 and 6 are given in table 1. The scatter plot of figure 8 demonstrates that the four pipes could almost be distinguished solely on the first two invariants. In practice three invariants reliably (up to two standard deviations) distinguish all the examples here.

| | *Invariant 1* | | *Invariant 2* | | *Invariant 3* | |
|---|---|---|---|---|---|---|
| | *mean* | *s.d.* | *mean* | *s.d.* | *mean* | *s.d.* |
| *pipe 1 (13)* | −21.988 | 0.1800 | 130.513 | 0.1671 | −22.531 | 0.1417 |
| *pipe 2 (6)* | −21.459 | 0.0998 | 129.530 | 0.1514 | −22.410 | 0.1938 |
| *pipe 3 (5)* | −23.981 | 0.1383 | 130.336 | 0.1564 | −22.089 | 0.1631 |
| *pipe 4 (12)* | −24.442 | 0.1879 | 130.042 | 0.1773 | −22.592 | 0.1781 |

Table 1: *Invariants computed using a Fisher linear discriminant based on the canonical frame measures shown in figure 7. The bracketted numbers after each pipe give the number of images contributed for that pipe to the computation of the Fisher Discriminant matrix.*

Figure 9: *viewpoint-invariant recognition. (a) The image contains one pipe in the model-library (centre left), and another that is not in the library, as well as other objects. (b) The pipe in the library is correctly recognised. The black curve shows the projected model symmetry set. All processing is automatic.*

# 6 Model Based Recognition

There are two stages in building a recognition system: first, acquisition, where canonical frame curves, and their invariants, are stored in a model library; second, recognition, where the system identifies which model (if any) is in a perspective image.

Recognition proceeds [22] by: (1) computing symmetry sets for all suitable curve pairs; (2) computing invariants for each symmetry set curve; (3) using the invariants as an *index* to access the model library—if an invariant value corresponds to one of the library values, a recognition hypothesis is generated; (4) verifying the recognition hypothesis by comparing the target symmetry set to a library curve.

A recognition system has been built which can identify a pipe from a perspective image. The image can contain several objects from the library as well as other unmodelled objects ('clutter'), and the viewpoint is unconstrained. At present the model library contains four pipes. A recognition example is shown in figure 9. We are currently enlarging the model library, and investigating invariants which are less occlusion sensitive.

# 7 Discussion

We have demonstrated a viewpoint-invariant representation for canal surfaces. The representation is stable over viewpoint, discriminates between objects, and can be reliably extracted from images. Invariants based on the representation have been successfully used as index functions in a model based recognition system.

Although theoretically correct only for precise envelopes of spheres, the methods are not too sensitive to deviations from the ideal. For example, the pipe cross-section is actually elliptical, with an aspect ratio varying between 0.89 and 1.0, rather than uniformly circular.

Other methods of extracting invariants from curves known up to a linear transformation will now be investigated. In particular, semi-differential curve invariants [26] do not require such a rich curve geometry as that required for a canonical frame (fewer inflections are needed).

**Acknowledgements** We are very grateful for discussions with Peter Giblin, who made a number of improvements to an earlier draft of this paper, and also to Bill Bruce and Andrew Blake. Financial support was provided by the EPSRC, ESPRIT Project 6448 'VIVA', and the University of Oxford.

# References

[1] Binford T.O., 'Inferring Surfaces from Images'. *Artificial Intelligence*, vol. 17, pp. 205–244, 1981.

[2] Binford T.O. and Levitt T.S., 'Quasi-Invariants: Theory and Explanation'. *Proc. Darpa IUW*, pp. 819–829, 1993.

[3] Blum H., 'Biological Shape and Visual Science (Part I)'. *J. theor. Biol.*, vol. 38, pp. 205–287, 1973.

[4] Brady M. and Asada H., 'Smoothed Local Symmetries and their Implementation'. *The International Journal of Robotics Research*, vol. 3, no. 3, pp. 36–61, 1984.

[5] Bruce J.W. and Giblin P.J. *Curves and Singularities.* Cambridge University Press, Second Edition, 1992.

[6] Burns J.B., Weiss R.S. and Riseman E.M., 'The Non-existence of General-case View-Invariants'. In [16].

[7] Canny J., 'A Computational Approach to Edge Detection'. *IEEE Trans. PAMI*, vol. 8, no. 6, pp. 679–698, 1986.

[8] Clemens D.T. and Jacobs D.W., 'Model Group Indexing for Recognition'. *IEEE Trans. PAMI*, vol. 13, no. 10, pp. 1007–1017, 1991.

[9] Duda R.O. and Hart P.E. *Pattern Classification and Scene Analysis.* Wiley, 1973.

[10] Forsyth D.A., Mundy J.L., Zisserman, A. and Rothwell C.A., 'Recognising rotationally symmetric surfaces from their outlines'. *Proc. ECCV*, LNCS 588, Springer-Verlag, 1992.

[11] Giblin P.J. and Brassett S.A., 'Local Symmetry of Plane Curves'. *American Mathematical Monthly*, vol. 92, no. 10, pp. 689–707, 1985.

[12] Kanade T., 'Recovery of Three Dimensional Shape of an Object from a Single View'. *Artificial Intelligence*, vol. 17, nos. 1–3, pp. 409–460, 1981.

[13] Lamdan Y., Schwartz J.T. and Wolfson H.J., 'Object Recognition by Affine Invariant Matching'. *Proc. CVPR*, pp. 335–344, 1988.

[14] Liu J.S., Mundy J.L., Forsyth D.A., Zisserman A. and Rothwell C.A., 'Efficient Recognition of Rotationally Symmetric Surfaces and Straight Homogeneous Generalized Cylinders', *Proc. CVPR*, 1993.

[15] Moses Y. and Ullman S., 'Limitations of Non Model-Based Recognition Systems'. *Proc. ECCV*, LNCS 588, Springer-Verlag, 1992.

[16] Mundy J.L. and Zisserman A.P., *Geometric Invariance in Computer Vision*. MIT Press, 1992.

[17] Mukherjee D.P., Zisserman A. and Brady J.M., 'Shape from symmetry—detecting and exploiting symmetry in affine images'. To appear, *Proc. Royal Soc.*, 1994.

[18] Pillow N., Utcke S. and Zisserman A., 'Viewpoint-Invariant Representation of Generalized Cylinders Using the Symmetry Set', Submitted for publication.

[19] Ponce J., 'Invariant properties of straight homogeneous generalized cylinders'. *IEEE PAMI*, vol. 11, no. 9, pp. 951–965, 1989.

[20] Pratt V., 'Direct Least-Squares Fitting of Algebraic Surfaces'. *Computer Graphics*, vol. 21, no. 4, pp. 145–151, 1987.

[21] Rothwell C.A., Zisserman A., Forsyth D.A. and Mundy J.L., 'Canonical Frames for Planar Object Recognition'. *Proc. ECCV*, LNCS 588, Springer-Verlag, 1992.

[22] Rothwell C.A., Zisserman A., Forsyth D.A. and Mundy J.L., 'Planar Object Recognition using Projective Shape Representation'. To appear, *IJCV*, 1994.

[23] Scott G.L., Turner S. and Zisserman A., 'Using a Mixed Wave/Diffusion Process to Elicit the Symmetry Set'. *Image and Vision Computing*, vol. 7, pp. 63–70, 1989.

[24] Springer C.E., *Geometry and Analysis of Projective Spaces*. Freeman, 1964.

[25] Ulupinar F., 'Perception of 3-D Shape from 2-D Image of Contours'. *PhD thesis, University of Southern California*, 1991.

[26] Van Gool L.J., Moons T., Pauwels E. and Oosterlinck A., 'Semi Differential Invariants'. In [16].

[27] Zerroug M. and Nevatia R., 'Using invariance and quasi-invariance for the segmentation and recovery of curved objects'. In LNCS 825, Springer-Verlag, 1994.